Barometric pumping of a fractured porous medium

V. V. Mourzenko, C. Varloteaux, S. Guillon, J. -F. Thovert, E. Pili, P. M. Adler

HAL Id: hal-01196402
https://hal.archives-ouvertes.fr/hal-01196402

Submitted on 17 Sep 2015

Barometric pumping of a fractured porous medium

V. V. Mourzenko[1], C. Varloteaux[2], S. Guillon[3,4], J.-F. Thovert[1], E. Pili[3,4], and P. M. Adler[2]

[1]Institut Pprime, CNRS, SP2MI, Futuroscope Chasseneuil, France, [2]UPMC Metis, Paris, France, [3]CEA, DAM, DIF, Arpajon, France, [4]Institut de Physique du Globe de Paris, Paris VII-Denis Diderot University, Paris, France

Abstract Barometric pumping plays a crucial role in the release of trace gases from fractured porous media to the atmosphere, and it requires a rigorous and complete modeling in order to go beyond the approximate schemes available in the literature. Therefore, a coupled set of convection and convection-diffusion equations for a slightly compressible fluid in unsteady conditions should be solved. The numerical methodology is presented, and it is applied to conditions close to the ones of the Roselend Natural Laboratory (France). The precision of the code is assessed and the mechanism of barometric pumping is explained. The usual schematization by simple vertical fractures is shown to be only qualitative. Finally, barometric pumping is shown to be efficient in a narrow range of parameter values; its efficiency is a decreasing function of the matrix porosity and of the fracture density.

1. Introduction

Fluctuations in the ambient atmospheric pressure result in motion of air in fractured porous media. This mechanism, known as barometric pumping, can efficiently transport gaseous species through the vadose zone to the atmosphere. This is of interest in many environmental and engineering fields as shown by the abundant literature and the review by *Kuang et al.* [2013]. Barometric pumping plays an important role in the remediation of contaminated sites, and it controls the exposure to radon in buildings. Pressure-driven airflow is responsible for the possible seepage of gases from a cavity to the atmosphere [*Nilson et al.*, 1991]. This latter feature is expected to play a central role in the detection of underground nuclear explosions [*Nilson et al.*, 1991; *Carrigan et al.*, 1996], and it is involved in seepage of CO_2 from carbon sequestration sites [*Oldenburg and Unger*, 2003]. In response to these challenges, a precise modeling of barometric pumping is needed for any kind of fractured porous media in order to make progress with respect to the approximate schemes developed up to now.

The formalism of flow through a porous medium from a cavity under the action of pressure variation is analogous to that of heat conduction in solids, which broadens its applicability to temperature variations. As stressed by *Nilson et al.* [1991], barometric pumping is enhanced by the presence of fractures, which permit pressure variations to propagate deeper than in porous media, to the order of 100 m. To date, barometric pumping has not been modeled for heterogeneous porous media with realistic shapes and distributions of fractures.

This paper is organized as follows. Section 2 presents the flow and convection-dispersion equations through fractured porous media. Section 3 provides the main results. Preliminary checks are reported first. Then, the phenomenon of barometric pumping is discussed, including a comparison with pure diffusion and configurations with vertical fractures. Some parametric studies on the influence of fracture density and porosity are detailed. These numerical simulations are conducted with parameter values relevant for the Roselend Natural Laboratory (Alps, France), where flow parameters of the crystalline rocks were determined [*Guillon et al.*, 2013; *Patriarche et al.*, 2007]. The influence of some other parameters such as the molecular diffusion coefficient, the fracture aperture, and the percolating character of the fracture network is summarized. A few concluding remarks and possible extensions are given in section 4.

2. General

This section addresses briefly single phase, slightly compressible flow through fractured porous media [*Adler et al.*, 2012]. Due to the specific transport properties of fractures, the flow through a naturally fractured porous medium differs drastically from that in a conventional porous medium. The key feature is that
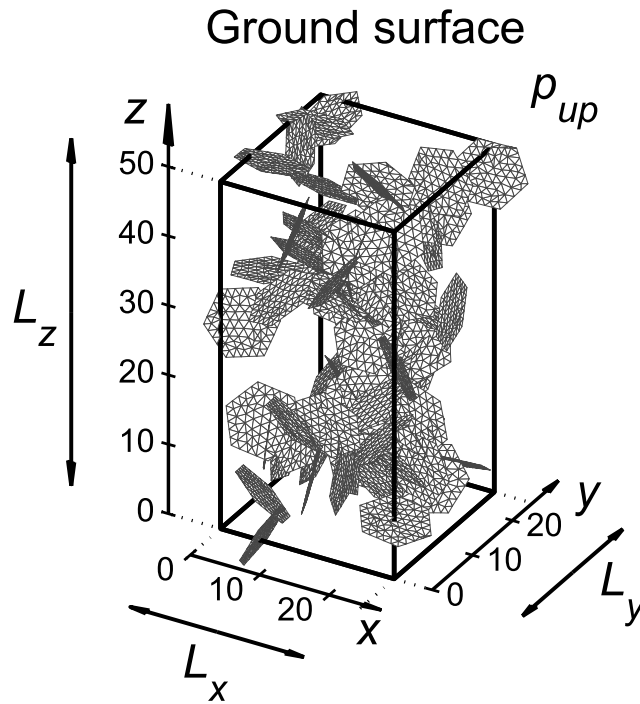
Ground surface

Figure 1. Scheme of the model and of the fracture mesh used for the simulations. The fracture network has a density $\rho = 1.86 \cdot 10^{-3}$ m^{-3} and a mesh size $\delta = R/4$ (see text for details).

in most cases the porous matrix provides the main storage for the fluids while transport takes place mainly through the fracture system.

The general situation is presented in Figure 1 where notations are given. A fractured porous medium of size $L_x \times L_y \times L_z$ is subjected to a sinusoidal pressure variation at its top $z = L_z$. At its bottom $z = 0$, a constant concentration $c = 1$ is maintained. The microscale Reynolds and Péclet numbers are assumed to be small with respect to 1 in the porous medium and the fractures; these assumptions are satisfied for the applications given in section 3.

The porous matrix has a bulk permeability K_m [L^2] which may vary with space. In the matrix, Darcy's law for the local seepage velocity $\bar{v}$ and the mass conservation for slightly compressible flow can be written as

$$\bar{v} = -\frac{K_m}{\mu}\nabla p \quad , \quad \varepsilon_m \, C_m \, \frac{\partial p}{\partial t} + \nabla \cdot \bar{v} = 0 \tag{1}$$

where t is the time, μ the viscosity of the gas, and p the pressure; ε_m is the air matrix porosity, and C_m the air compressibility. If $\varepsilon_m C_m$ is constant, a matrix pressure diffusivity D_{pm} can be defined and (1) can be written as a diffusion equation for the pressure

$$\frac{\partial p}{\partial t} - \nabla \cdot \left(D_{pm}\nabla p\right) = 0 \quad , \quad D_{pm} = \frac{K_m}{\mu \varepsilon_m C_m} \tag{2}$$

When the resistance to normal flow can be neglected, the hydraulic properties of a fracture can be characterized by its transmissivity σ [L^3] which relates the in-plane flow rate $\mathbf{J}$ to the surface pressure gradient $\nabla_s p$ [*Adler et al.*, 2012]

$$\mathbf{J} = -\frac{\sigma}{\mu}\nabla_s p \tag{3}$$

For illustration, the fracture can be viewed as a plane channel of aperture b. Then, the classical Poiseuille law yields the transmissivity σ

$$\sigma = \frac{b^3}{12} \tag{4}$$

The continuity equation for the flow through such a fracture reads as

$$b \, C_f \frac{\partial p}{\partial t} + \nabla_s \cdot \mathbf{J} = [\bar{v}] \cdot \mathbf{n} \tag{5}$$

where $[\bar{v}]$ denotes the jump of the seepage velocity in the porous medium across the fracture and C_f is the compressibility of the gas in the fracture. Again, if bC_f is constant in a fracture, a pressure diffusivity D_f can be defined, and (5) is written as

$$\frac{\partial p}{\partial t} - \nabla_s \cdot (D_f \nabla_s p) = \frac{[\bar{v}] \cdot \boldsymbol{n}}{b \, C_f} \quad , \quad D_f = \frac{\sigma}{b \, \mu C_f} \tag{6}$$

The assumptions of uniform $\varepsilon_m C_m$ and bC_f used to write down the diffusion equations (2) and (6) are by no means a requirement for the numerical model. At this point, notations can be simplified; C_m and C_f are equal to C; ε_m is denoted by ε.

The tracer transported by the gas is assumed to be chemically passive. Hence, in a medium of porosity ε, the mass balance equation for the tracer concentration c^* reads

$$\frac{\partial (\varepsilon c^*)}{\partial t} + \nabla \cdot (\overline{\mathbf{v}} c^*) - D_m \nabla \cdot \left(\overline{D}_{pm} \nabla c^* \right) = 0 \tag{7}$$

where D_m is the molecular diffusion coefficient and $\overline{D}_{pm}$ the effective conductivity of the porous medium.

In the fractures, c^* is regarded as constant across the fracture aperture; because of continuity, it is equal to c^* in the matrix on either side (i.e., $[c^*] = 0$). The mass balance reads

$$\frac{\partial (bc^*)}{\partial t} + \nabla_s \cdot (\mathbf{J}c^*) - D_m \nabla_s \cdot \left(\Sigma \nabla_s c^* \right) + \left[\left(\overline{\mathbf{v}} c^* - \overline{D}_{pm} D_m \nabla c^* \right) \right] \cdot \mathbf{n} = 0 \tag{8}$$

where Σ is the fracture conductivity; for a channel of constant width b, Σ is equal to b [*Adler et al.*, 2012]. Gaseous tracer flux continuity at the fracture/matrix interfaces is built in equation (8) through the exchange term.

This system of equations should be also supplemented with constitutive equations for at least the effective conductivity $\overline{D}_{pm}$. Archie's law is supposed to hold

$$\overline{D}_{pm} = \varepsilon^{1.4} \tag{9}$$

Boundary conditions are as follows. The fracture network, the fluid flow, and the concentration are supposed to be spatially periodic along the horizontal x and y axes. On the bottom and top layers, the following conditions are imposed

$$z = 0 : \quad \text{zero fluid flux} \; , \quad c(x, y, 0, t) = 1 \tag{10a}$$

$$z = L_z : \quad p(x, y, L_z, t) = p_a + \Delta p \sin(\omega t) \; , \quad c(x, y, L_z, t) = 0 \tag{10b}$$

where p_a is the mean surface pressure (Pa), Δp the amplitude of the pressure fluctuations (Pa), and ω its pulsation (s^{-1}).

The initial conditions are the following. Flow calculations are made independently; after a few periods, the pressure field undergoes periodic variations. The convection-diffusion equation is solved for these periodic flow variations. Initially, $c(x, y, z, 0)$ is equal to zero everywhere for $z > 0$.

The equations are solved in the following way. The fractures and the porous medium are meshed by triangles and tetrahedra of sides smaller than a given size δ. The equations are discretized by the finite volume technique and solved by conjugate gradient methods. Numerical dispersion in the convection-diffusion equations is diminished by a flux-limiting scheme. A particular attention is paid to the exchanges between the fractures and the surrounding porous medium.

Finally, the previous equations can be used in a stationary state in order to derive an estimation of the macroscopic permeability $\overline{K}$ and of the macroscopic diffusion coefficient $\overline{D}_{fpm}^*$ of the fractured porous medium. The 3-D, time-dependent concentration field can be compared to the one-dimensional analytical solution of pure diffusion in a uniform porous medium [*Carslaw and Jaeger*, 1959]

$$c_{an}^*(z, t) = \text{erfc} \left[0.5z \left(\overline{D}_{fpm}^* t \right)^{-1/2} \right] \tag{11}$$

3. Results

3.1. Parameters and Preliminary Checks

The barometric pressure parameters chosen in this paper are

$$\omega = 10^{-5} s^{-1} \quad , \quad \Delta p = 10^3 \, Pa \tag{12}$$

They represent variations in weather patterns at the Roselend site [*Guillon et al.*, 2013]. The molecular diffusion coefficient is taken as

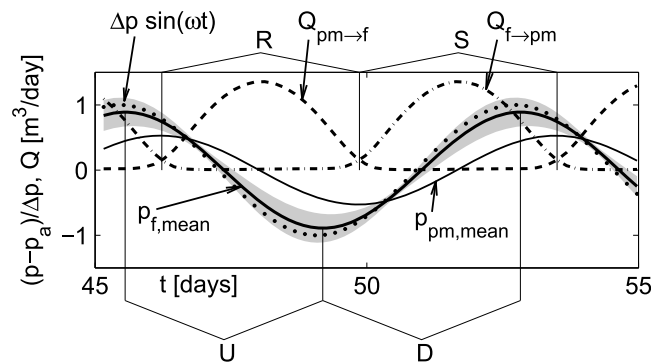$$D_m = 10^{-6} \, m^2 s^{-1} \tag{13}$$

Figure 2. Analysis of barometric pumping. Data are for the conditions (12)–(14). The imposed pressure variation $\Delta p \sin(\omega t)$ is indicated by the dotted line; $p_{f,mean}$ is the mean-normalized pressure in the matrix, $Q_{f \to pm}$ the flow rate from fractures to matrix, and $Q_{pm \to f}$ from matrix to fractures. Four periods can be distinguished for the tracer movements: storage (S) into the matrix and restitution (R) to the fractures; up (U) and down (D) in the fracture network. Shaded area indicates standard deviation of the fracture pressure spatial variations.

This value compares with the order of magnitude of diffusion coefficients for most gaseous tracers [*Marrero and Mason*, 1972]. As for the transport parameters, air viscosity, compressibility coefficient, matrix permeability, and porosity are taken as

$$\mu = 2 \cdot 10^{-5} \text{ Pa s}, \quad C = 10^{-5} \text{ Pa}^{-1},$$
$$K_m = 10^{-16} \, m^2, \quad \varepsilon = 0.01$$
$$(14)$$

following *Guillon et al.* [2013]. The fracture network properties were determined from the stereological analysis of fractures observed in the Roselend tunnel [*Patriarche et al.*, 2007]. The fractures are supposed to be hexagonal, and the radius of the circumscribed disk is $R = 5$ m. The fracture aperture is $b = 5 \cdot 10^{-4}$ m; therefore, the dimensionless fracture transmissivity $\sigma' = \sigma / (K_m R)$ [*Adler et al.*, 2012] is equal to $2.013 \cdot 10^4$. The number of fractures per cubic meter is chosen to be equal to $\rho = 1.86 \, 10^{-3}$ m^{-3} which is just above the percolation threshold. Two other fracture networks of densities $4.85 \, 10^{-3}$ and $9.7 \, 10^{-3}$m^{-3} are studied as well for sensitivity analysis.

The size of the unit cell is $25 \times 25 \times 50$ m^3, as recalled in Figure 1. Its vertical dimension corresponds roughly to the Roselend site.

As a preliminary check, numerical simulations were conducted in an unfractured porous medium. The results agree very well with the one-dimensional solution $c_{an}^*(z, t)$ (11) down to a concentration of 10^{-5}.

3.2. Illustration of the Barometric Pumping
The key features of barometric pumping as a transport mechanism are explained in Figure 2. The mean pressure $p_{f,mean}$ in the fractures, obtained by averaging pressure over all the fractures, closely follows the barometric pressure variations indicated by the dotted line. $p_{f,mean}$ has been smoothed; the shaded area indicates standard deviation of the fracture pressure spatial variations. The pressure averaged over all the matrix $p_{pm,mean}$ has also been smoothed; as expected, $p_{pm,mean}$ is out of phase and of smaller amplitude than $p_{f,mean}$.

Two periods can be distinguished, namely, up (U) and down (D), when tracer migrates upward (respectively, downward) in the fracture network, following the sign of the time derivative of $p_{f,mean}$ (Figure 2).

The gas flow rates from the fractures to the porous medium $Q_{f \to pm}$ and from the porous medium to the fractures $Q_{pm \to f}$ were calculated and are presented in Figure 2. Two other periods can be distinguished, namely, storage (S) in the porous medium, when $Q_{f \to pm}$ is positive, and restitution (R) to the fractures when $Q_{pm \to f}$ is positive. $Q_{f \to pm}$ is significant when the mean pressure in the fractures is larger than the mean pressure in the matrix, and it is otherwise equal to zero. However, there is a phase shift between this flow rate and the mean pressure difference since the exchange rate depends on the fast-responding matrix pressure near the fractures, whereas the variations of $p_{pm,mean}$ are delayed. Analogous comments can be done for $Q_{pm \to f}$.

The succession of tracer transport up and down the fractures (U,D) combined with tracer storage and restitution, in and out the matrix (S, R) is characteristic of barometric pumping; this stepwise and irreversible effect, also called ratcheting effect [*Nilson et al.*, 1991], results in enhanced migration toward the surface.

The concentration field of the gaseous tracer, calculated during 98 days, is represented in Figure 3. A very important characteristic is that the gaseous tracer reaches the surface rapidly compared to the purely diffusive case. Gaseous tracer concentration at the surface ($z = 50$ m) is of the order of 10^{-5} after 50 days (Figure 3d), while diffusion leads to this concentration only at 5 m from the source.
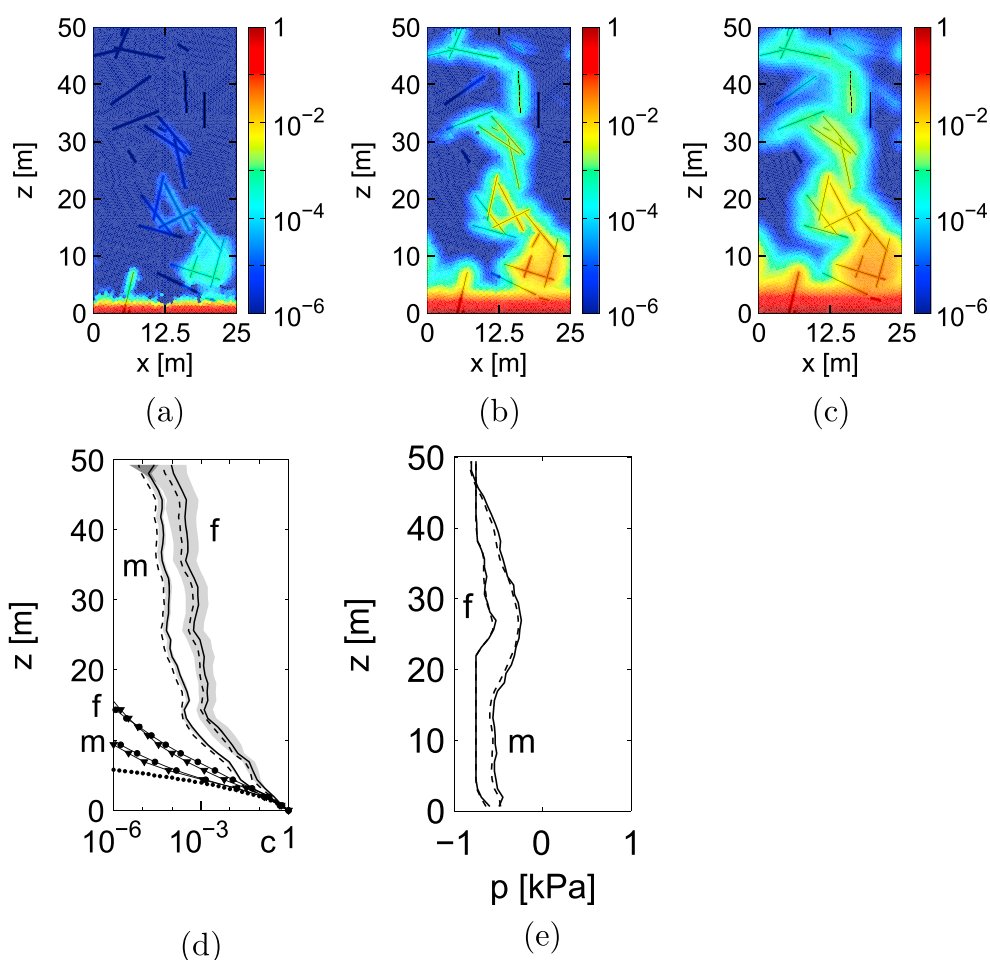
Figure 3. Barometric pumping in a fractured porous medium with a density $\rho = 1.86\,10^{-3}$ m^{-3} and a matrix porosity $\epsilon = 0.01$. The concentration field after (a) 10, (b) 50, and (c) 98 days. The (d) concentration and (e) pressure averaged over horizontal sections are shown at 50 days in the matrix and the fractures (solid lines marked m and f, respectively); concentration and pressure profiles obtained with a finer mesh $\delta = R/8$ correspond to the dashed lines. The concentration profiles in Figure 3d are averaged over one period, with grey areas indicating the ranges of variations of the gaseous tracer concentrations. The dotted line in Figure 3d shows the analytical 1-D diffusion solution $c^*_{an}(z,t)$. Symbols show the concentration profiles for a single vertical fracture with an equivalent overall permeability ($b = 2.9 \cdot 10^{-4}$ m, ▼) or an equivalent macroscopic diffusion coefficient ($b = 1.26 \cdot 10^{-3}$ m, ●).

Close to the source ($z \leq 5$ m) where concentration is high, transport is controlled by diffusion and the concentration depends mostly on z as shown by Figure 3d. Further from the source, barometric pumping is the controlling transport mechanism, and the concentration shows a limited dependence on z.

The concentration averaged over a section appears to always be higher in the fractures than in the porous matrix (Figure 3d). This is due to the ratcheting effect.

Since the pressure fluctuations driving migration are acting at the surface while the tracer source is at depth, only the fractures that do percolate are used as a preferential path for tracer migration. Therefore, barometric pumping is a very efficient transport mechanism, even in very complex fracture networks, the tracer being shortly connected with the surface.

3.3. Parametric Studies

Some preliminary checks were performed first. For $\rho = 1.86\,10^{-3}$ m^{-3}, two simulations were conducted, with mesh sizes $\delta = 0.25\,R$ and $0.125\,R$; after 50 days, the average pressures and the average concentrations are very close whatever δ (Figures 3d and 3e). Configurations with a single fracture or repeated parallel vertical fractures [e.g., *Nilson et al.*, 1991], which were extensively used for semianalytical models, were calculated with the same values of the parameters as for the fracture network, except b which is chosen in such a way
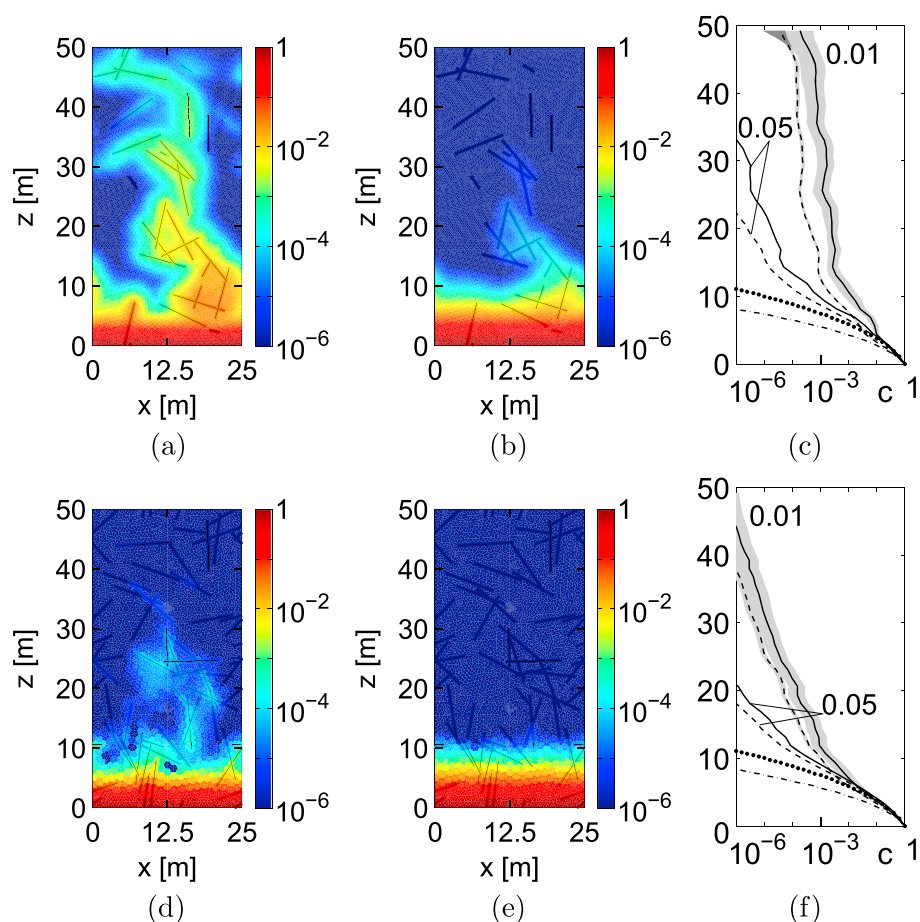
Figure 4. Influence of the fracture density and matrix porosity. Data are for a fractured porous medium with (a–c) $\rho = 1.86\,10^{-3}$ and (d–f) $4.85\,10^{-3}$ m^{-3}, and for $\epsilon = 0.01$ (Figures 4a and 4d) and 0.05 (Figures 4b and 4e) after 98 days. In Figures 4c and 4f the averaged concentration profiles in the matrix (dashed lines) and in the fractures (solid lines) are shown for $\epsilon = 0.01$ and 0.05, as indicated by numbers. The concentration profiles are averaged over one period, grey areas indicate the ranges of variations of the gaseous tracer concentrations during one period. The dash-dotted and dotted lines in Figures 4c and 4f show the 1-D analytical solution $c_{an}^*(z, t)$ (11) with $\overline{D}_{fpm}^*$ calculated for $\epsilon = 0.01$ and 0.05, respectively.

that the media with a single fracture and the network have either the same macroscopic permeability or the same macroscopic diffusion coefficient. Concentration for a single fracture is seen to be much smaller than the values obtained for the fracture network (Figure 3d). Therefore, using fracture networks with realistic shapes is required in order not to underestimate the efficiency of barometric pumping.

A nonpercolating network could be generated for the same density $\rho = 1.86\,10^{-3}$ m^{-3}. The difference with the concentration fields shown in Figure 3 is spectacular, since the concentration profile is practically one-dimensional and completely controlled by diffusion.

Evolutions with time for the three fracture densities $\rho = 1.86\,10^{-3}$, $4.85\,10^{-3}$, and $9.7\,10^{-3}$ m^{-3} were analyzed, and only the first two are shown in Figure 4. For $\rho = 1.86\,10^{-3}$ m^{-3}, the tracer quickly finds and follows the preferential connected fracture path, and it reaches the top of the medium within 98 days (Figure 4a). Simultaneously, the concentration increases in a quasi one-dimensional way at the bottom of the medium and around the preferential connected fracture path. When ρ increases, the preferential path tends to disappear (Figure 4d). The tracer migrates by diffusion until transport in the fracture network is initiated. For $\rho = 9.7\,10^{-3}$ m^{-3}, this trend is more pronounced and the concentration field follows the 1-D diffusion solution.

Two values of matrix porosities, namely, ϵ=0.01 and 0.05, were also studied for the networks with $\rho = 1.86\,10^{-3}$ m^{-3} (Figures 4a–4c) and $4.85\,10^{-3}$ m^{-3} (Figures 4d–4f). Archie's law (9) implies that the

effective conductivity is multiplied by a factor of 10 when porosity increases from 0.01 to 0.05. When porosity is increased while K_m and σ remain the same, the fluid fluxes are not changed. However, it results in a larger storage effect in the matrix, reducing the efficiency of barometric pumping. An increase in porosity has a similar effect as an increase in fracture density since both diminish the transport efficiency by barometric pumping.

Other calculations were performed which cannot be detailed in this letter. The influence of the molecular diffusion coefficient, of the fracture aperture, and of the matrix permeability were studied. The conclusion is always the same; when transport in the porous matrix is too large, barometric pumping is suppressed and the overall behavior is diffusive as shown in Figure 4e. Another test was performed with a network of density $\rho = 1.86\,10^{-3}$ m^{-3} which did not percolate along any of the three dimensions; flow and transport are considerably diminished and the overall behavior is again diffusive.

Therefore, the efficiency of barometric pumping appears to be controlled by the ratio $\mathcal{R}$ of the gaseous tracer transfers through the network and from the fractures into the matrix. When $\mathcal{R}$ is too small, the behavior of the fractured porous medium is diffusive.

4. Conclusion

Barometric pumping can be simulated for complex discrete fracture networks embedded in a porous matrix. A detailed qualitative and quantitative description of this mechanism is made. This can be applied to situations where release of gas to the atmosphere could be a threat such as in the safety assessment of carbon sequestration; moreover, quantitative predictions of gas emission following an underground nuclear test are highly desirable. Transport by barometric pumping is most efficient for a limited range of parameter values. The fracture network must be connected; an increase in the matrix porosity or in the fracture density results in a decrease in the barometric pumping efficiency. The qualitative discussion of the possible crucial influence of the ratio $\mathcal{R}$ should be made more quantitative.

This initial study can be extended in many ways. The properties of the porous matrix and of the fractures can be varied at will since every mesh element may be given different properties. Morever, the boundary conditions which are spatially periodic in the horizontal plane can be changed. Calculations can also be made with measured pressure fluctuations at the ground surface. Finally, as the formalism of pressure-driven flow is similar to that of heat conduction in solids, these developments can also be extended to temperature variations.

References

Adler, P. M., J.-F. Thovert, and V. V. Mourzenko (2012), *Fractured Porous Media*, Oxford Univ. Press, Oxford, U. K.
Carrigan, C. R., R. A. Heinle, G. B. Hudson, J. J. Nitao, and J. J. Zucca (1996), Trace gas emissions on geological faults as indicators of underground nuclear testing, *Nature*, *382*, 528–531.
Carslaw, H. S., and J. C. Jaeger (1959), *Conduction of Heat in Solids*, Oxford Univ. Press, Oxford, U. K.
Guillon, S., M. T. Vu, E. Pili, and P. M. Adler (2013), Field and numerical determinations of pneumatic flow parameters of unsaturated fractured porous rocks on various scales, *Water Resour. Res.*, *49*, 2801–2811, doi:10.1002/wrcr.20263.
Kuang, X., J. J. Jiao, and H. Li (2013), Review on airflow in unsaturated zones induced by natural forcings, *Water Resour. Res.*, *49*, 6137–6165, doi:10.1002/wrcr.20416.
Marrero, T. R., and E. A. Mason (1972), Gaseous diffusion coefficients, *J. Phys. Chem. Ref. Data*, *1*, 3–118.
Nilson, R. H., E. W. Peterson, K. H. Lie, N. R. Burkhard, and J. R. Hearst (1991), Atmospheric pumping: A mechanism causing vertical transport of contaminated gases through fractured permeable media, *J. Geophys. Res.*, *96*, 21,933–21,948.
Oldenburg, C. M., and A. J. A. Unger (2003), On leakage and seepage from geologic carbon sequestration sites: Unsaturated zone attenuation, *Vadose Zone J.*, *2*, 287–296.
Patriarche, D., E. Pili, P. M. Adler, and J.-F. Thovert (2007), Stereological analysis of fractures in the Roselend tunnel and permeability determination, *Water Resour. Res.*, *43*, W09421, doi:10.1029/2006WR005471.